A Centrosymmetric Matrix Based Technique for the Interpolation of a Hermitian Signal

By

Magdy Tawfik Hanna
Dept. of Engineering Mathematics and Physics
Cairo University / Fayoum Branch
Fayoum
Egypt

Sana Ahmed Mansoori
Dept. of Electrical Engineering
University of Bahrain
State of Bahrain

The Contact Author:

Magdy Tawfik Hanna
Email: hanna@ieee.org

Abstract

This work is concerned with the signal interpolation problem, i.e., given only samples of a signal, a method is derived for evaluating its samples on finer grids. The derivation is based on a discrete-time decimation formula. In the special case where the known samples have the Hermitian property, two schemes are presented and mathematically proved to result in interpolated points having the same property. The first scheme does not utilize the known sample at the origin and results in a square system of equations to be solved for the unknown interpolated points of the signal. The second scheme has the merit of utilizing all the known samples, but it results in an overdetermined system of equations to be solved by the least squares method. The exploitation of the elegant properties of the involved centrosymmetric matrices is central to the treatment presented here.

Keywords: Interpolation, Hermitian signal, centrosymmetric matrix, discrete-time decimation.

Mathematical Subject Classification: 15A57, 41A05, 94A12, 15A06

I. Introduction

Starting from a discrete-time decimation formula, an interpolation method for a bandlimited signal is proposed. More specifically, given only the samples $\psi(k_1 T)$ of a signal $\psi(t)$ corresponding to a sampling period T, the technique generates the samples $\psi\left(\left(k_1 + \frac{k_2}{a_0^m}\right)T\right)$ for $k_2 = 1, \ldots, (a_0^m - 1)$ – where a_0 and m are positive integers and $a_0 > 1$ - corresponding to a sampling period $D = \frac{T}{a_0^m}$. The larger the value of the integer m, the finer the interpolation points will be. Figure 1 illustrates the layout of the given and interpolated samples for the case of $a_0 = 2$ and $m = 2$. The special case where the known samples have the Hermitian property, namely $\psi(-nT) = \psi^*(nT)$, is treated in detail and two schemes are proposed and mathematically proved to result in interpolated samples having the same property. One scheme does not utilize the known sample $\psi(0)$ and results in a square system of equations to be solved for the unknown interpolated points of $\psi(t)$. A second scheme utilizes all the known samples and results in an overdetermined system of equations to be solved by the least squares method. Exploiting the elegant properties of the involved centrosymmetric matrices proves the fact that the interpolated samples have the Hermitian property.

In section II the general case of an arbitrary signal is considered and the proposed interpolation method is developed based on a discrete-time decimation formula. In section III the two schemes pertaining to the special case of a Hermitian signal are presented. In section IV some simulation results are demonstrated showing the superiority of the second scheme.

II. The General Case: Interpolation of an Arbitrary Signal

Let $\psi(t)$ be a bandlimited signal and assume that only its samples corresponding to the sampling period T are known. It is required to find the samples corresponding to the higher sampling rate, i.e., the smaller sampling period $\frac{T}{a_0^m}$ where a_0 and m are positive integers. The problem can be mathematically stated as: Given the sequence

$$\psi[n] = \psi(nT) \tag{1}$$

find the interpolated sequence

$$\psi_m[n] = \psi\left(n\frac{T}{a_0^m}\right). \tag{2}$$

These sequences are related by

$$\psi[n] = \psi_m\left[a_0^m n\right] . \tag{3}$$

Therefore the given sequence $\psi[n]$ can be regarded as a decimated version of the required sequence $\psi_m[n]$ with a decimation ratio a_0^m. Using the available results on sampling discrete-time signals and decimation, referring to Fig.2 (a,b) and assuming that $\alpha < \pi$, one concludes that the discrete-time Fourier transforms of $\psi[n]$ and $\psi_m[n]$ are related [1] by

$$\Psi(e^{j\omega}) = \frac{1}{a_0^m}\Psi_m\left(e^{j\frac{\omega}{a_0^m}}\right) \qquad |\omega| \le \pi . \tag{4}$$

Taking the inverse transform of both sides of the above equation, one gets

$$\psi[n] = \frac{1}{2\pi}\int_{-\pi}^{\pi}\frac{1}{a_0^m}\Psi_m\left(e^{j\frac{\omega}{a_0^m}}\right)e^{j\omega n}d\omega . \tag{5}$$

Using the definition of the discrete-time Fourier transform, the above equation reduces to

$$\psi[n] = \frac{1}{a_0^m}\frac{1}{2\pi}\int_{-\pi}^{\pi}e^{j\omega n}\sum_{k\in Z}\psi_m[k]e^{-j\frac{\omega}{a_0^m}k}d\omega . \tag{6}$$

Interchanging the order of integration and summation results in

$$\psi[n] = \frac{1}{a_0^m}\sum_{k\in Z}\psi_m[k]\frac{1}{2\pi}\int_{-\pi}^{\pi}e^{j\omega\left(n-\frac{k}{a_0^m}\right)}d\omega \tag{7}$$

Performing the above integration and using the sinc function [2]

$$\mathrm{sinc}(x) = \frac{\sin(\pi x)}{\pi x} , \tag{8}$$

one gets

$$\psi[n] = \frac{1}{a_0^m}\sum_{k\in Z}\psi_m[k]\mathrm{sinc}\left(n-\frac{k}{a_0^m}\right). \tag{9}$$

Since for any integer p,

$$\mathrm{sinc}(p) = \begin{cases} 1 & p = 0 \\ 0 & p \neq 0 \end{cases}, \tag{10}$$

equation (9) reduces to

$$a_0^m \psi[n] = \psi_m\left[a_0^m n\right] + \sum_{k \neq n a_0^m} \psi_m[k]\,\mathrm{sinc}\left(n - \frac{k}{a_0^m}\right), \tag{11}$$

and upon utilizing (3), the above equation simplifies to

$$\left(a_0^m - 1\right)\psi[n] = \sum_{k \neq n a_0^m} \psi_m[k]\,\mathrm{sinc}\left(n - \frac{k}{a_0^m}\right). \tag{12}$$

Using equations (1) and (2), the above equation can be expressed as

$$\sum_{k \neq n a_0^m} \psi\left(k\frac{T}{a_0^m}\right)\mathrm{sinc}\left(n - \frac{k}{a_0^m}\right) = \left(a_0^m - 1\right)\psi(nT). \tag{13}$$

This is the key formula to be exploited for evaluating $\psi(t)$ at $t = \frac{kT}{a_0^m}$, $k \neq p a_0^m$, (p integer) given $\psi(t)$ at t = nT. Expressing the integer k as

$$k = k_1 a_0^m + k_2 \tag{14}$$

and noticing that $k \neq p a_0^m$ implies that $k_2 \neq 0$, Eq. (13) can be rewritten as

$$\sum_{k_1 = k_{1\min}}^{k_{1\max}-1} \sum_{k_2 = 1}^{a_0^m - 1} \psi\left(\left(k_1 + \frac{k_2}{a_0^m}\right)T\right)\mathrm{sinc}\left(n - k_1 - \frac{k_2}{a_0^m}\right) = \left(a_0^m - 1\right)\psi(nT) \tag{15}$$

where it has been assumed that the contribution to the left hand side of ψ(t) values outside the range, $k_{1\min}\ T < t < k_{1\max}\ T$, is negligible. In order to evaluate the $\left(a_0^m - 1\right)\left(k_{1\max} - k_{1\min}\right)$ unknowns appearing on the left hand side of (15), one should write that equation for the same number of values of n in order to get a square linear system of algebraic equations to be solved for $\psi\left(\left(k_1 + \frac{k_2}{a_0^m}\right)T\right)$, $k_2 = 1, \ldots, (a_0^m - 1)$ and $k_1 = k_{1\min}, \ldots, k_{1\max} - 1$. For numerical stability the range of n values should include the range of k_1 values in the middle.

In the simple case of $a_0 = 2$ and m = 1, Eq. (15) reduces to

$$\sum_{k_1 = k_{1\min}}^{k_{1\max}-1} \psi\left(\left(k_1 + \frac{1}{2}\right)T\right)\mathrm{sinc}\left(n - k_1 - \frac{1}{2}\right) = \psi(nT). \tag{16}$$

Here there is only one unknown for each sampling interval; namely the value of ψ(t) at the midpoint of the interval. Consequently the number of unknowns is just $\left(k_{1\max} - k_{1\min}\right)$ and one can take the set of n values to be identical to that of the k_1 values.

Given ψ(t) at the sampling instants $t = k_1 T$, computing $\psi\left(\left(k_1 + \frac{k_2}{2^m}\right)T\right)$, $k_2 = 1, \cdots, \left(2^m - 1\right)$ to any required degree of subdivision can be accomplished using either of the following two methods:

One) Apply Eq. (15) to find all the fractional points of ψ(t) in one step by solving a large system of $\left(2^m - 1\right)\left(k_{1\max} - k_{1\min}\right)$ equations.

Two) Apply Eq. (16) on m stages starting by the given values for T, k_{1min} and k_{1max} to find ψ(t) at t = (k_1 + 0.5)T; interlace these values with those of ψ(t) at t = k_1T and use the resulting set on the right hand side of (16) in the next stage after halving T and doubling k_{1min} and k_{1max} .

III. The Special Case: Interpolation of a Hermitian Signal

Some signals like the Morlet wavelet have the Hermitian property [3,4], namely,

$$\psi(-t) = \psi^*(t). \tag{17}$$

Here the support of ψ(t) is symmetric and (15) takes the form

$$\sum_{k=-K}^{K-1} \sum_{r=1}^{a_0^m - 1} \psi\left(\left(k + \frac{r}{a_0^m}\right)T\right) \operatorname{sinc}\left(n - k - \frac{r}{a_0^m}\right) = \left(a_0^m - 1\right)\psi(nT). \tag{18}$$

The number of fractional points of ψ(t) to be evaluated is 2N where

$$N = L\,K \tag{19}$$

and

$$L = \left(a_0^m - 1\right). \tag{20}$$

In what follows two schemes will be presented for finding the 2N interpolated points of ψ such that they will inherit the Hermitian property of the known samples $\psi(nT)$ of the signal $\psi(t)$. In the first scheme exactly 2N values of n symmetrically located with respect to the origin are substituted in (18), i.e., n = -N, … , -2,-1,1,2, … ,N where n = 0 has been excluded. The advantage of having a square system of 2N equations to be solved for the 2N unknowns is to be considered versus the disadvantage of introducing a gap at n = 0 in the sequence of known samples. In the second scheme (2N + 1) values of n symmetrically located with respect to the origin are substituted in (18), i.e., n = -N, … ,-1,0,1, … ,N. The advantage of utilizing all the known samples of $\psi(nT)$ is to be assessed versus the disadvantage of having a minimally overdetermined system of (2N + 1) equations in 2N unknowns.

III.A The First Scheme

The 2N values n = -N, … ,-1,1, … ,N (where n = 0 has been excluded) are substituted in (18) and the resulting 2N constraints are arranged in matrix form to get

$$Ax = y \tag{21}$$

where

$$y = \left(a_0^m - 1\right)\left[\psi(-NT) \quad \cdots \quad \psi(-T) \quad \psi(T) \quad \cdots \quad \psi(NT)\right]^T \tag{22}$$

and x is the 2K-partitioned vector

$$x = \left[x_{-K} \quad \cdots \quad x_{-1} \quad x_0 \quad x_1 \quad \cdots \quad x_{K-1}\right]^T \tag{23}$$

with the k-th partition being the $(a_0^m - 1)$-dimensional vector

$$x_k = \left[\psi\left(\left(k + \frac{1}{a_0^m}\right)T\right) \quad \psi\left(\left(k + \frac{2}{a_0^m}\right)T\right) \quad \cdots \quad \psi\left(\left(k + \frac{a_0^m - 1}{a_0^m}\right)T\right)\right]^T . \tag{24}$$

The square matrix A of order 2N in (21) can be expressed as the partitioned matrix

$$A = \begin{pmatrix} P & Q \\ R & S \end{pmatrix} \tag{25}$$

where the square matrices P, Q, R, and S of order N are the N x K partitioned matrices defined by

$$P = \begin{bmatrix} F_{-N,-K} & F_{-N,-(K-1)} & \cdots & F_{-N,-1} \\ F_{-(N-1),-K} & F_{-(N-1),-(K-1)} & \cdots & F_{-(N-1),-1} \\ \vdots & \vdots & \ddots & \vdots \\ F_{-1,-K} & F_{-1,-(K-1)} & \cdots & F_{-1,-1} \end{bmatrix}, \tag{26}$$

$$S = \begin{bmatrix} F_{1,0} & F_{1,1} & \cdots & F_{1,(K-1)} \\ F_{2,0} & F_{2,1} & \cdots & F_{2,(K-1)} \\ \vdots & \vdots & \ddots & \vdots \\ F_{N,0} & F_{N,1} & \cdots & F_{N,(K-1)} \end{bmatrix}, \tag{27}$$

$$Q = \begin{bmatrix} F_{-N,0} & F_{-N,1} & \cdots & F_{-N,(K-1)} \\ F_{-(N-1),0} & F_{-(N-1),1} & \cdots & F_{-(N-1),(K-1)} \\ \vdots & \vdots & \ddots & \vdots \\ F_{-1,0} & F_{-1,1} & \cdots & F_{-1,(K-1)} \end{bmatrix}, \tag{28}$$

$$R = \begin{bmatrix} F_{1,-K} & F_{1,-(K-1)} & \cdots & F_{1,-1} \\ F_{2,-K} & F_{2,-(K-1)} & \cdots & F_{2,-1} \\ \vdots & \vdots & \ddots & \vdots \\ F_{N,-K} & F_{N,-(K-1)} & \cdots & F_{N,-1} \end{bmatrix}. \tag{29}$$

The above four partitioned matrices have been expressed in terms of the $(a_0^m - 1)$ - dimensional row vector $F_{p,q}$ defined by

$$F_{p,q} = \left[\operatorname{sinc}\left(p - q - \frac{1}{a_0^m}\right) \quad \operatorname{sinc}\left(p - q - \frac{2}{a_0^m}\right) \quad \cdots \quad \operatorname{sinc}\left(p - q - \frac{a_0^m - 1}{a_0^m}\right)\right] . \tag{30}$$

In the special case of $a_0 = 2$ and $m = 1$, the vector $F_{p,q}$ reduces to a scalar.

Theorem 1

Matrix A defined by (25) with P, Q, R, and S defined by (26)-(29) is centrosymmetric.

Proof:

Vector $F_{p,q}$ defined by (30) is a function of the difference (p-q); moreover,

$$F_{p,q} = F_{-q,-p} \ . \tag{31}$$

Postmultiplying $F_{p,q}$ by the contra-identity matrix J_L of order L defined by

$$J_L = \begin{pmatrix} & & 1 \\ & \iddots & \\ 1 & & \end{pmatrix}, \tag{32}$$

where L is given by (20), one obtains

$$\begin{aligned} F_{p,q} J_L &= \left[\operatorname{sinc}\left(p-q-\frac{a_0^m-1}{a_0^m} \right) \quad \cdots \quad \operatorname{sinc}\left(p-q-\frac{2}{a_0^m} \right) \quad \operatorname{sinc}\left(p-q-\frac{1}{a_0^m} \right) \right] \\ &= \left[\operatorname{sinc}\left(q+1-p-\frac{1}{a_0^m} \right) \quad \cdots \quad \operatorname{sinc}\left(q+1-p-\frac{a_0^m-2}{a_0^m} \right) \quad \operatorname{sinc}\left(q+1-p-\frac{a_0^m-1}{a_0^m} \right) \right]. \end{aligned} \tag{33}$$

By comparing (33) and (30) it is obvious that

$$F_{p,q} J_L = F_{q+1,p} = F_{q,p-1} \ . \tag{34}$$

Expressing J_{2N} in the partitioned form

$$J_{2N} = \begin{pmatrix} 0 & J_N \\ J_N & 0 \end{pmatrix} \tag{35}$$

and using (25) for A results in

$$J_{2N} A J_{2N} = \begin{pmatrix} J_N S J_N & J_N R J_N \\ J_N Q J_N & J_N P J_N \end{pmatrix} \ . \tag{36}$$

Premultiplying S of (27) by J_N and postmultiplying it by the same matrix expressed in the partitioned form

$$J_N = \begin{pmatrix} & & J_L \\ & \iddots & \\ J_L & & \end{pmatrix} \tag{37}$$

leads to

$$J_N S J_N = \begin{bmatrix} F_{N,(K-1)} J_L & \cdots & F_{N,1} J_L & F_{N,0} J_L \\ \vdots & \ddots & \vdots & \vdots \\ F_{2,(K-1)} J_L & \cdots & F_{2,1} J_L & F_{2,0} J_L \\ F_{1,(K-1)} J_L & \cdots & F_{1,1} J_L & F_{1,0} J_L \end{bmatrix} . \tag{38}$$

Using the regular matrix notation, the (i,j) partition of the above matrix is given by

$$\left[J_N S J_N\right]_{i,j} = F_{N-i+1,K-j} J_L \qquad , \text{i} = 1 , \ldots , \text{N} \quad , \quad \text{j} = 1 , \ldots , \text{K} \tag{39}$$

and upon utilizing (34) it reduces to

$$\left[J_N S J_N\right]_{i,j} = F_{K-j,N-i} \quad . \tag{40}$$

Similarly the (i,j) partition of matrix P of (26) is given by

$$\left[P\right]_{i,j} = F_{-N+i-1,-K+j-1} \quad . \tag{41}$$

Applying property (31) and calling to remembrance that $F_{p,q}$ is a function of only $(p-q)$, the above equation can be reexpressed as

$$\begin{aligned} \left[P\right]_{i,j} &= F_{-N+i,-K+j} \\ &= F_{K-j,N-i} \end{aligned} \tag{42}$$

From (40) and (42) one concludes that

$$\left[J_N S J_N\right]_{i,j} = \left[P\right]_{i,j} \qquad , \text{i} = 1 , \ldots , \text{N} \quad , \quad \text{j} = 1 , \ldots , \text{K} \tag{43}$$

and hence

$$J_N S J_N = P \quad . \tag{44}$$

Using the fact that

$$JJ = I \tag{45}$$

where I is the identity matrix, one concludes from (44) that

$$J_N P J_N = S \quad . \tag{46}$$

By the same token it can be proved that

$$J_N R J_N = Q \tag{47}$$

and consequently

$$J_N Q J_N = R \quad . \tag{48}$$

Substituting (44), (46) - (48) into (36) and comparing with (25) one gets

$$J_{2N} A J_{2N} = A \quad . \tag{49}$$

Therefore matrix A is centrosymmetric [5]. (Q.E.D.)

Since the known samples of ψ(t) satisfy the Hermitian property

$$\psi(-nT) = \psi^*(nT) , \tag{50}$$

the vector y defined by (22) is a Hermitian vector, i.e.,

$$Jy^* = y \quad . \tag{51}$$

Taking the complex conjugate of both sides of (21), noticing that matrix A is real, premultiplying by J_{2N} and using property (45) of the contra-identity matrix, one obtains

$$\left(JAJ\right)\left(Jx^*\right) = Jy^* \quad . \tag{52}$$

Upon utilizing (49) and (51) one gets

$$AJx^* = y \quad . \tag{53}$$

Assuming the nonsingularity of matrix A, (21) and (53) result in

$$Jx^* = x\,. \tag{54}$$

Therefore the solution vector x of (21) is a Hermitian vector which implies that the interpolated values of ψ(t) satisfy the Hermitian property as desired.

III.B The Second Scheme

Writing (18) for n = -N, … ,-1,0,1, … ,N and arranging the resulting (2N+1) equations in matrix form, one gets

$$Bx = z \tag{55}$$

where the vector of unknowns x is defined by (23) and (24) and where z is the $(2N+1)$-dimensional vector

$$z = \left(a_0^m - 1\right)\left[\psi(-NT) \quad \cdots \quad \psi(-T) \quad \psi(0) \quad \psi(T) \quad \cdots \quad \psi(NT)\right]^T. \tag{56}$$

The (2N+1) x 2N matrix B in (55) is the partitioned matrix

$$B = \begin{bmatrix} P & Q \\ f & g \\ R & S \end{bmatrix} \tag{57}$$

where the four square matrices P, Q, R, and S of order N are the same as in (26)-(29) and the N-dimensional row vectors f and g are defined by

$$f = \left\lfloor F_{0,-K} \quad F_{0,-(K-1)} \quad \cdots \quad F_{0,-1} \right\rfloor, \tag{58}$$

$$g = \left\lfloor F_{0,0} \quad F_{0,1} \quad \cdots \quad F_{0,(K-1)} \right\rfloor \tag{59}$$

with vector $F_{p,q}$ defined by (30).

Theorem 2

Matrix B defined by (57) is centrosymmetric.

Proof:

Pre- and postmultiplying B by the contra-identity matrices J_{2N+1} and J_{2N} respectively, one gets

$$J_{2N+1}BJ_{2N} = \begin{pmatrix} & & J_N \\ & 1 & \\ J_N & & \end{pmatrix} B \begin{pmatrix} & J_N \\ J_N & \end{pmatrix} \tag{60}$$

and upon substituting (57) one obtains

$$J_{2N+1}BJ_{2N} = \begin{pmatrix} J_N S J_N & J_N R J_N \\ gJ_N & fJ_N \\ J_N Q J_N & J_N P J_N \end{pmatrix}. \tag{61}$$

Expressing J_N as the partitioned matrix (37) and using (59), one gets

$$gJ_N = \left\lfloor F_{0,(K-1)}J_L \quad \cdots \quad F_{0,1}J_L \quad F_{0,0}J_L \right\rfloor \tag{62}$$

and upon applying (34), one obtains

$$gJ_N = \begin{bmatrix} F_{K,0} & \cdots & F_{2,0} & F_{1,0} \end{bmatrix}. \tag{63}$$

By virtue of (31), the above row vector reduces to

$$gJ_N = \begin{bmatrix} F_{0,-K} & \cdots & F_{0,-2} & F_{0,-1} \end{bmatrix} \tag{64}$$

and consequently (58) and (64) lead to

$$gJ_N = f \ . \tag{65}$$

Postmultiplying both sides of the above equation by J_N and applying (45) one obtains

$$fJ_N = g \ . \tag{66}$$

Substituting (44), (46), (47), (48), (65) and (66) in (61) and comparing with (57) one finally concludes that

$$J_{2N+1} B J_{2N} = B \ . \tag{67}$$

Therefore matrix B is centrosymmetric[1].

(Q.E.D.)

The least squares solution vector x_{LS} of (55) can be computed from the normal equations [6],

$$B^T B x_{LS} = B^T z \ . \tag{68}$$

By virtue of (67) and (45) it follows that

$$\begin{aligned} J_{2N} B^T B J_{2N} &= \left(J_{2N} B^T J_{2N+1}\right)\left(J_{2N+1} B J_{2N}\right) \\ &= \left(J_{2N+1} B J_{2N}\right)^T \left(J_{2N+1} B J_{2N}\right) \\ &= B^T B . \end{aligned} \tag{69}$$

Therefore, the square matrix of coefficients of the normal equations (68) is centrosymmetric. Taking the complex conjugate of both sides of (68), noticing that B is real, premultiplying by J_{2N} and using (45), one gets

$$\left(J_{2N} B^T B J_{2N}\right) J_{2N} x_{LS}^* = \left(J_{2N} B^T J_{2N+1}\right) J_{2N+1} z^* \ . \tag{70}$$

The definition (56) of vector z and the Hermitian property (50) lead to

$$J_{2N+1} z^* = z \ . \tag{71}$$

Substituting (67), (69) and (71) in (70) one gets

$$B^T B\left(J_{2N} x_{LS}^*\right) = B^T z \tag{72}$$

[1]Here the definition of a centrosymmetric matrix given in [5] for a square matrix has been extended to a rectangular matrix.

If matrix B of (57) has a full column rank of 2N, the matrix $B^T B$ will be nonsingular and consequently the least squares solution vector x_{LS} in (68) will be unique. Therefore (68) and (72) lead to

$$J_{2N} x_{LS}^{*} = x_{LS} \tag{73}$$

This property of the least squares solution vector of the overdetermined system of equations (55) implies that the interpolated values of the signal $\psi(t)$ will have the Hermitian property as desired.

The interpolation technique presented in this paper has been inspired by the scaling operation of the wavelet theory where $\psi\left(\frac{t}{a_0^m}\right)$ is obtained from the mother wavelet $\psi(t)$ by scaling [3,4]. When compared to the popular spline interpolation technique [7,8], the present method has the advantage of a reduced computational load since there is no need for first finding the coefficients of each spline segment joining every pair of successive points and second substituting the values of the intermediate points in order to get the interpolated samples. The present method also has an elegant matrix formulation of the problem – involving a centrosymmetric matrix – that leads to a formal proof that the interpolated samples will have the Hermitian property should the given samples have it.

IV. Simulation Results

Two examples are presented for the interpolation of a Hermitian signal given only a finite set of its samples. In the first example the signal, namely the Shannon wavelet, is exactly bandlimited but its rate of decay in the time domain is slow. In the second example the signal, namely the Morlet wavelet, is not exactly bandlimited although its rates of decay in both the time and frequency domains are sufficiently high.

Example 1:

The Shannon wavelet shown in Fig. 3a, is defined by [3]:

$$\psi(t) = \frac{\sin(\pi t/2)}{\pi t/2}\cos(3\pi t/2) \tag{74}$$

and its continuous-time Fourier transform shown in Fig. 3b is given by:

$$\Psi(\Omega) = \begin{cases} 1 & \pi < |\Omega| < 2\pi \\ 0 & \text{otherwise} \end{cases} \tag{75}$$

The Nyquist sampling frequency for this bandlimited signal is 4π rad/sec and the corresponding sampling period is T = 0.5 sec. For the purpose of testing the interpolation schemes presented in the previous section, only the 17 samples – shown in Fig. 4 – corresponding to the Nyquist rate will be assumed known, i.e., the values of the signal beyond |t| = 4 sec will be considered negligible. This signal is interpolated to get 2^4 - 1 = 15 additional samples between every pair of the given samples by halving the sampling interval 4 times since

it has been found experimentally that implementation method (b) mentioned at the end of section II has better numerical behavior than implementation method (a) mentioned there. The two interpolation schemes of section III are applied and the resulting interpolated signals are shown in Fig. 5a,b respectively. The corresponding interpolation error – defined as the difference between the interpolated signal and the exact one of (74) – is plotted for both schemes in Fig. 6a,b respectively.

In this example the apparent inferiority of the first interpolation scheme – based on excluding the middle sample $\psi(0)$ in a quest for a square system of equations – to the second scheme can be attributed to two reasons. Mainly, the signal does not decay fast enough in the time domain and consequently it is not sufficient to use only samples confined to $|t| \leq 4$ for the purpose of interpolation. Secondarily, the number of assumed known samples of 17 is small and excluding the middle sample in the first scheme explains the large interpolation error around t = 0 in Fig. 6a. Interestingly, the second interpolation scheme exhibits a satisfactory performance although it is based on the approximate least squares solution of an overdetermined system of equations. The relatively large interpolation error towards the ends of the interval $-4 \leq t \leq 4$ in Fig. 6b is expected since no known samples have been assumed to exist beyond |t| = 4.

Example 2:

The Morlet wavelet shown in Fig. 7a is defined by

$$\psi(t) = e^{-0.5t^2} e^{j\Omega_0 t} \tag{76}$$

and its continuous-time Fourier transform – shown in Fig. 7b – is given by

$$\Psi(\Omega) = \sqrt{2\pi} e^{-0.5(\Omega-\Omega_0)^2} \tag{77}$$

See [3]. Since $\Psi(\Omega)$ is not bandlimited in the strict sense, its band edge (cutoff frequency) Ω_c will be taken to be the value of Ω at which $|\Psi(\Omega)|$ drops to ε of its peak value at $\Omega = \Omega_0$. It is straightforward to show that

$$\Omega_c = \Omega_0 + \sqrt{-2\ln\varepsilon} \tag{78}$$

and consequently the sampling period T should satisfy

$$T < \frac{\pi}{\Omega_c} \ . \tag{79}$$

Although $\psi(t)$ is not strictly time-limited, its support will be practically taken as $|t| \leq t_c$ where t_c is the time at which $|\psi(t)|$ drops to ε of its peak value of $\psi(0) = 1$. It is obvious that

$$t_c = \sqrt{-2\ln\varepsilon} \ . \tag{80}$$

For the purpose of this example the center frequency $\Omega_0 = 2\pi$ rad/sec and the tolerance parameter ε = 0.001 will be used. Equations (78)-(80) result in Ω_c = 10 rad/sec, T < 0.314

second and t_c = 3.717 seconds respectively. Taking T = 0.25 second and the support of $\psi(t)$ to be $|t| \le 4$ results in the 33 samples shown in Fig. 8 and regarded as the only known samples of this signal. Applying both interpolation schemes of the last section to generate 2^4 - 1 = 15 additional samples between every pair of given samples by halving the sampling interval 4 times as has been done in the previous example, one gets the interpolated signals of Fig. 9a,b where only the real parts are plotted. By comparing these two figures with the exact Morlet wavelet of Fig. 7a, it is obvious that both interpolation schemes produce quite satisfactory results. A careful examination of the corresponding interpolation errors shown in Fig. 10a,b reveals the relative merit of the second scheme. The main reason for the interpolation results of the present example to obviously outperform those of the previous one is that the Morlet wavelet decay fast enough in the time domain so that samples in the interval $-4 \le t \le 4$ are enough for the purpose of signal reconstruction. This rapid decay in the time domain of the Morlet wavelet – not exhibited by the Shannon wavelet – has more than counterbalanced the fact that it is not strictly bandlimited.

It should be mentioned that when the two implementation methods mentioned at the end of section II were tried in the above two examples it was found that method (a) suffers numerical instability because the involved matrix becomes ill-conditioned for m > 1. Actually all the simulation results presented here – for both interpolation schemes – were obtained by implementation method (b).

The second interpolation scheme of section III involving a minimally overdetermined system of equations – where the number of equations exceeds the number of unknowns by just one – has been shown to give better results when compared to the first scheme involving a square system of equations. Consequently one might be tempted to employ a more overdetermined system of equations with the objective of decreasing the interpolation error. This suggestion corresponds to including equations containing $\psi(nT)$ values as right hand sides of (16) for n values outside the region where the interpolation is taking place. A careful consideration of the details of the numerically stable implementation method (b) reveals that this suggestion is not tractable since at each stage the interpolated samples $\psi((k_1 + 0.5)T)$ should be interlaced with the given samples $\psi(k_1 T)$ and consequently the $\psi(nT)$ values to be used as right hand sides of (16) should lie in the same region where the interpolation is taking place, i.e., the system of equations should only be minimally overdetermined. The intuitive motivation behind the above suggestion is getting more information about the shape of the signal $\psi(t)$ by using more function values. The proper accommodation of this idea is to enlarge the region where the interpolation is taking place. This can be done by decreasing $k_{1\min}$ and increasing $k_{1\max}$ in (16) and consequently using a larger range of n values, i.e., incorporating more values

$\psi(nT)$ of the signal $\psi(t)$. In order to experimentally test this idea, example 2 above was repeated with $|t| \le 5$ (instead of $|t| \le 4$) as the support of $\psi(t)$ while fixing the remaining parameters. The corresponding interpolation errors for the two processing schemes are shown in Fig. 11a, b. By comparing Figs. 10a and 11a, one notices the decrease of the interpolation error. The same conclusion holds when comparing Figs. 10b and 11b.

V. Conclusion

Two interpolation schemes have been proposed for the reconstruction of a Hermitian signal given its samples. The first scheme ignores the middle sample in a quest for a square system of linear equations to be solved for the interpolated points. The second scheme retains all known samples and necessitates the use of the least squares approximate solution of an overdetermined system of equations. The simulation results reveal the superiority of the second scheme.

REFERENCES

[1] A.V. Oppenheim and A.S. Willsky with I.T. Young, *Signals and Systems*, Prentice-Hall, Englewood Cliffs, N.J., 1983.

[2] R.N. Bracewell, *The Fourier Transform and its Applications*, 2nd ed., McGraw-Hill, New York, 1986.

[3] Y.T. Chan, *Wavelet Basics*, Kluwer Academic Publishers, Boston, MA, 1995.

[4] M. Vetterli and J. Kovacevic, *Wavelets and Subband Coding*, Prentice-Hall, Englewood Cliffs, N.J., 1995.

[5] P.A. Roebuck and S. Barnett, "A survey of Toeplitz and related matrices," *International Journal of Systems Sciences*, vol. 9, no. 8, 1978, pp. 921-934.

[6] G.W. Stewart, *Introduction to Matrix Computations*, Academic Press, New York, 1973.

[7] S.C. Chapra and R.P. Canale, Numerical Methods for Engineers, 2nd Edition, McGraw-Hill, New York, 1989.

[8] M.L. James, G.M. Smith and J.C. Wolford, Applied Numerical Methods for Digital Computation, 4th Edition, Harper Collins College Publishers, New York, 1993.

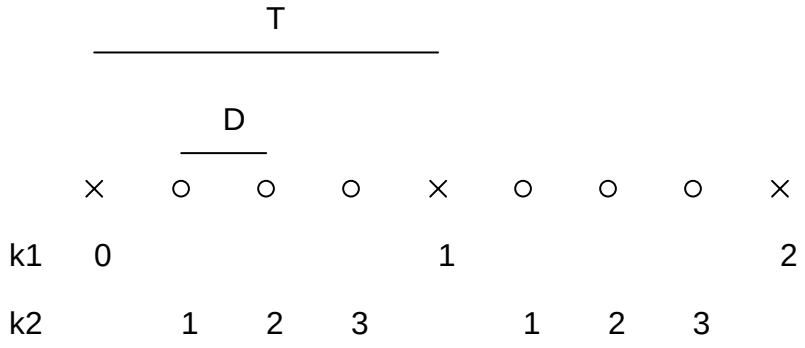

Fig. 1: The given and interpolated samples of $\psi(t)$.
(x : given sample , o : interpolated sample)

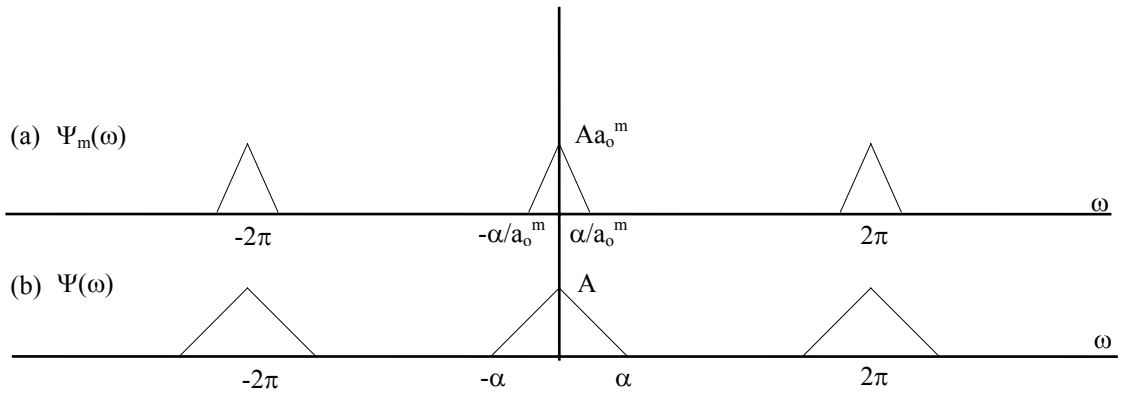

Fig. 2: A frequency domain illustration of the relation between $\Psi_m(e^{j\omega})$ and $\Psi(e^{j\omega})$.

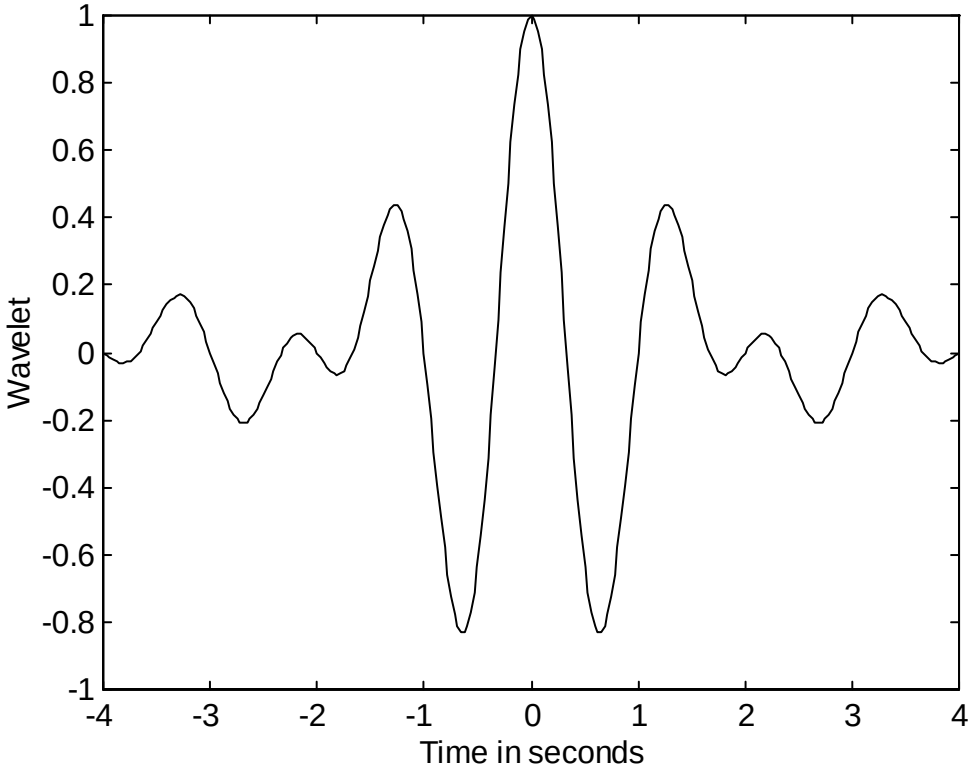

Fig. 3a: The Shannon wavelet $\psi(t)$.

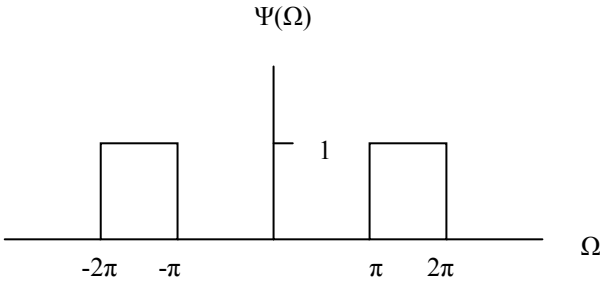

Fig. 3b: The continuous-time Fourier transform $\Psi(\Omega)$ of the Shannon wavelet $\psi(t)$.

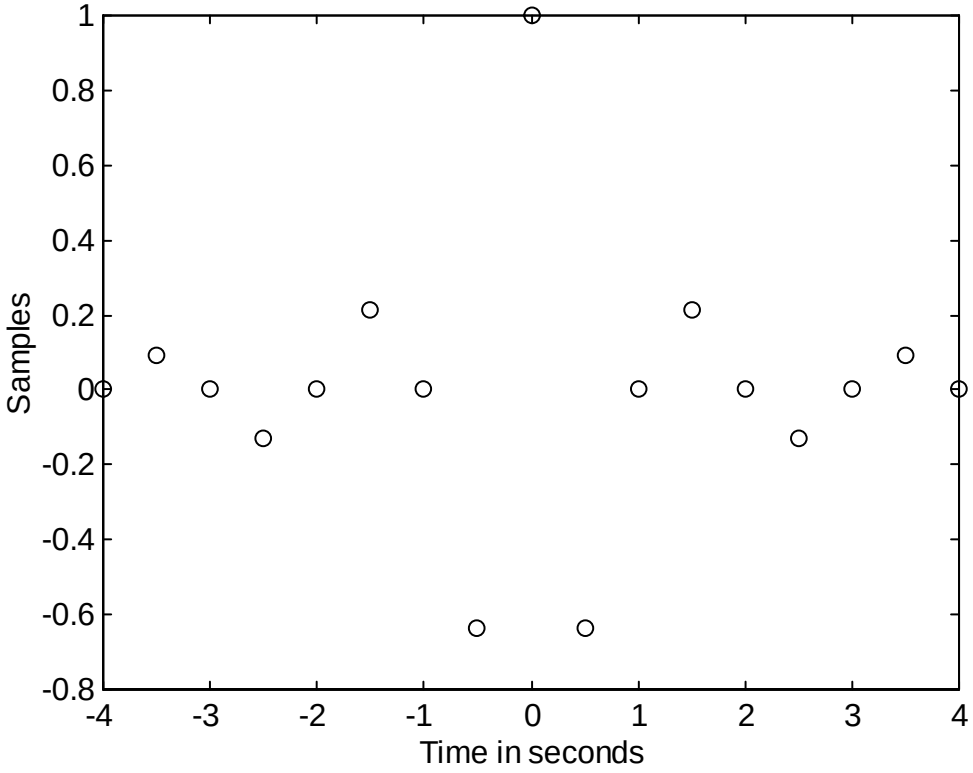

Fig. 4: The given samples of the Shannon wavelet.

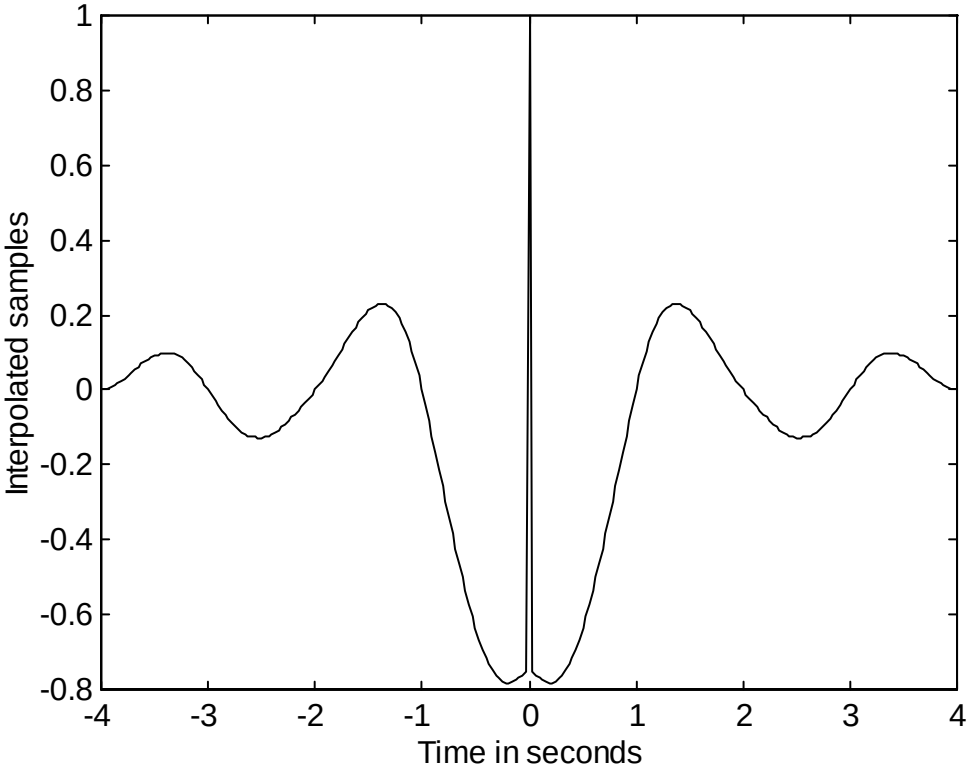

Fig. 5a: The interpolated Shannon wavelet using the first scheme.

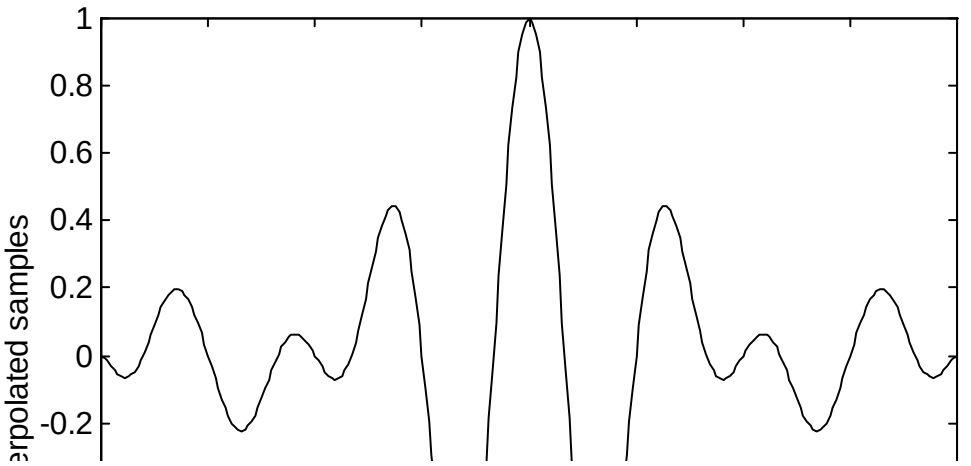

Fig. 5b: The interpolated Shannon wavelet using the second scheme.

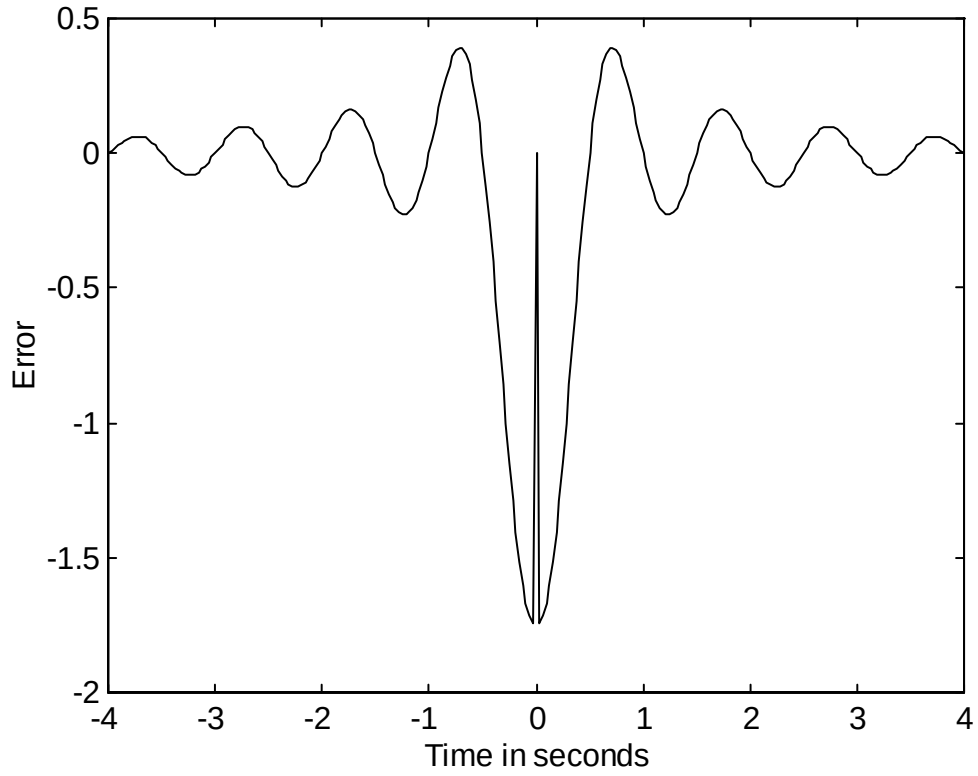

Fig. 6a: The interpolation error for the Shannon wavelet in the first scheme.

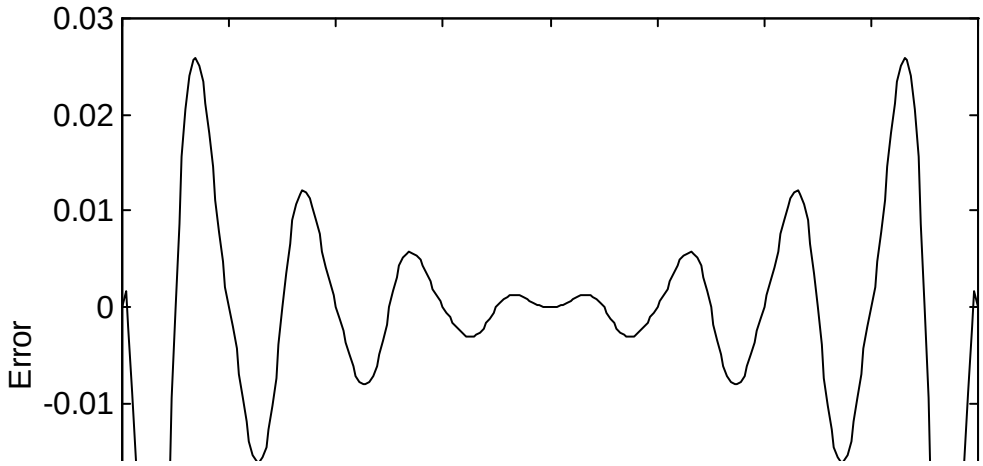

Fig. 6b: The interpolation error for the Shannon wavelet in the second scheme.

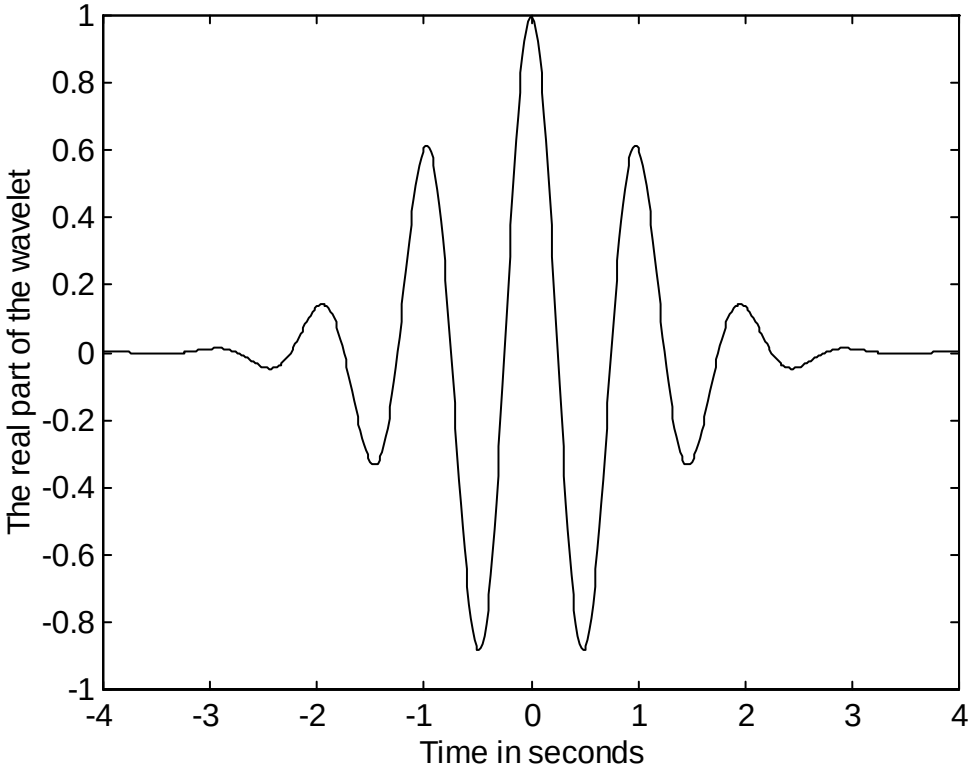

Fig. 7a: The Morlet wavelet $\psi(t)$.

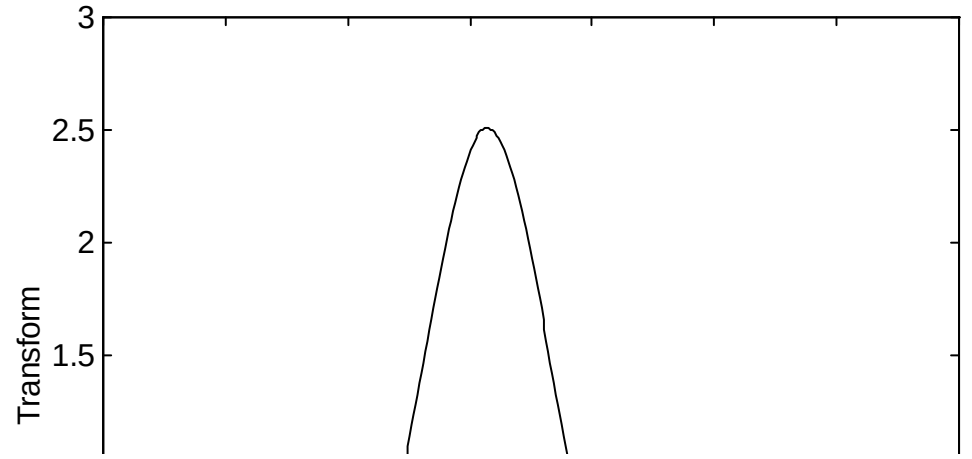

Fig. 7b: The continuous-time Fourier transform $\Psi(\Omega)$ of the Morlet wavelet $\psi(t)$.

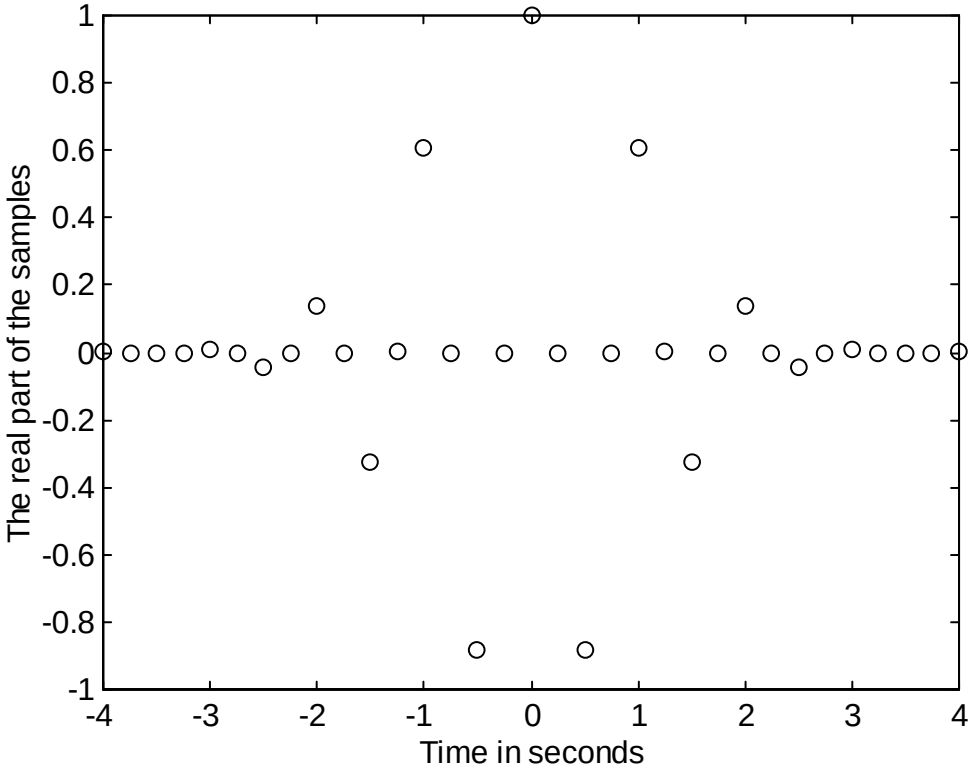

Fig. 8: The given samples of the Morlet wavelet.

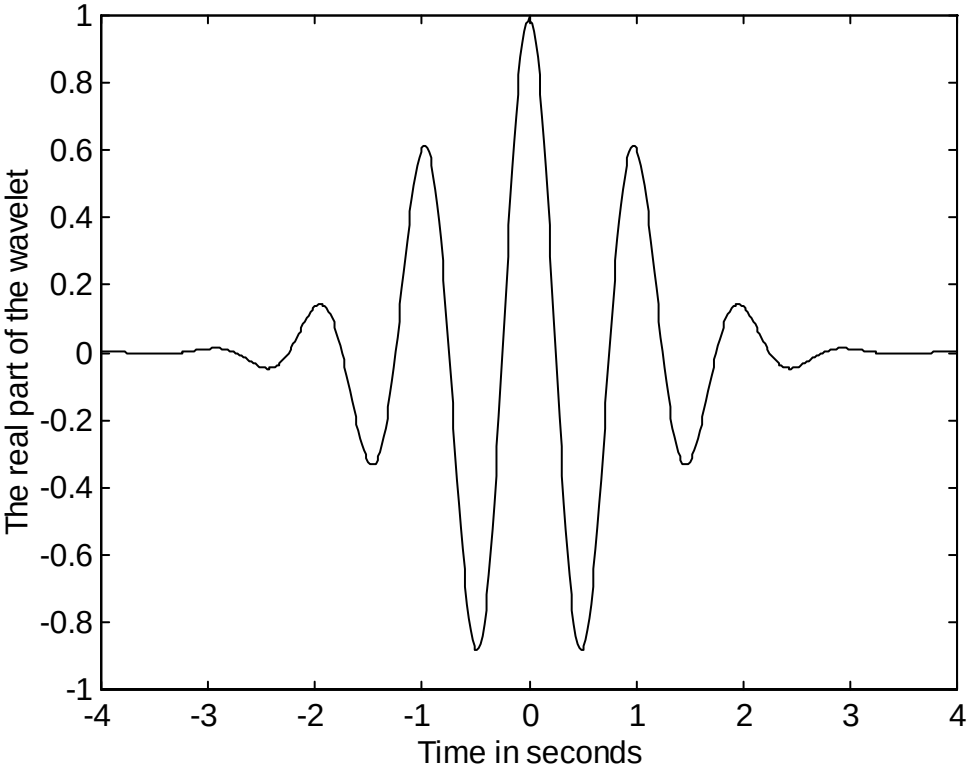

Fig. 9a: The interpolated Morlet wavelet using the first scheme for $|t| \leq 4$.

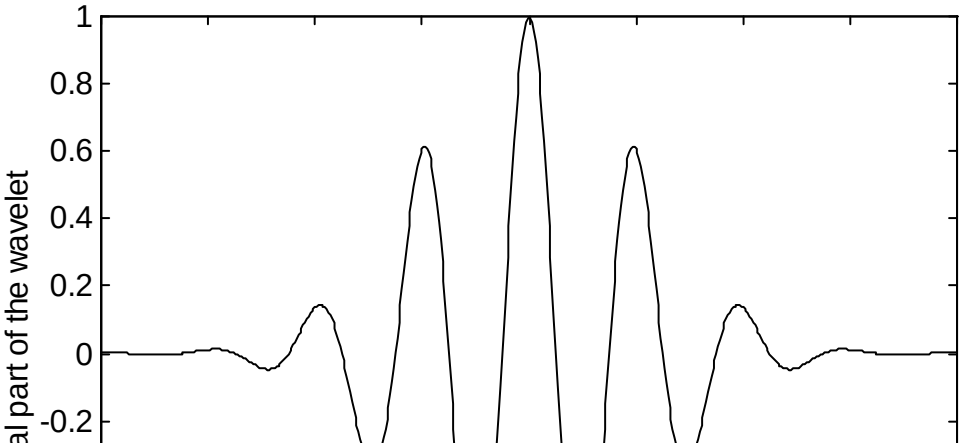

Fig. 9b: The interpolated Morlet wavelet using the second scheme for $|t| \leq 4$.

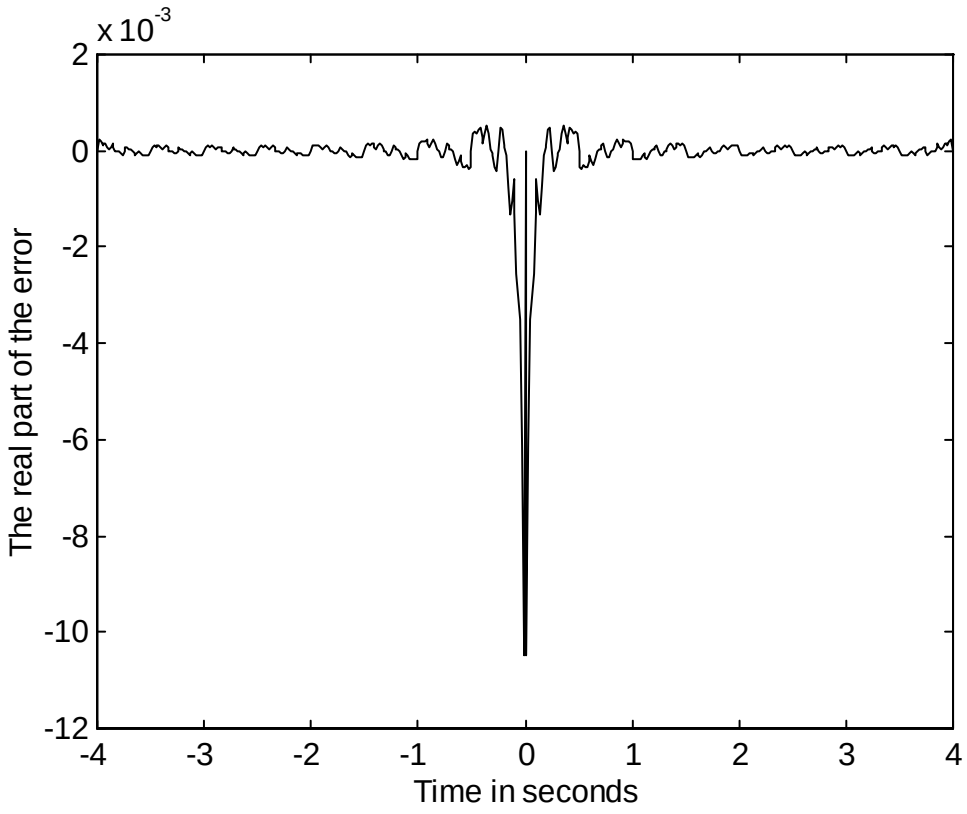

Fig. 10a: The interpolation error for the Morlet wavelet in the first scheme for $|t| \le 4$.

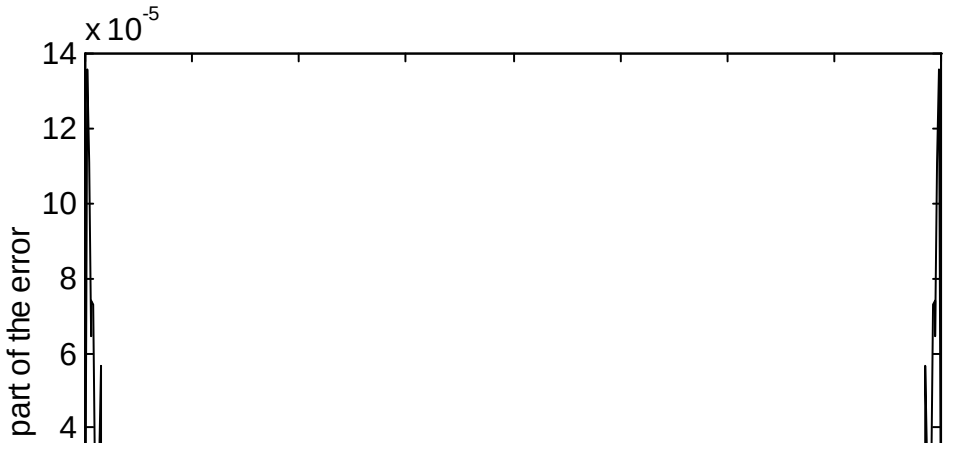

Fig. 10b: The interpolation error for the Morlet wavelet in the second scheme for $|t| \le 4$.

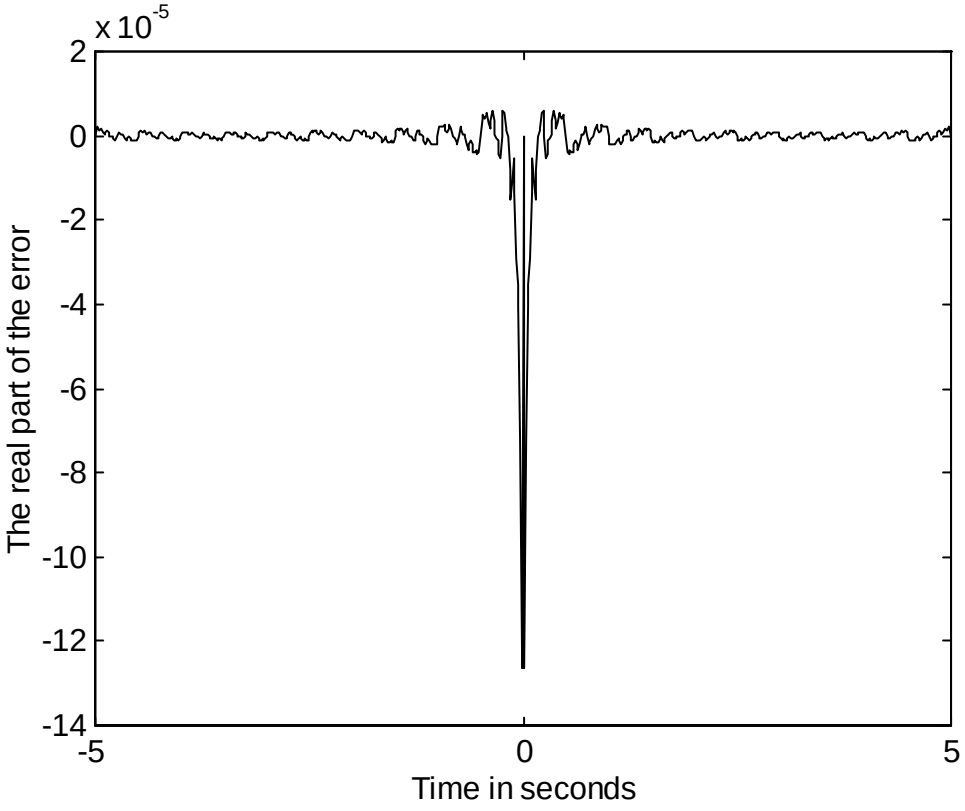

Fig. 11a: The interpolation error for the Morlet wavelet in the first scheme for $|t| \le 5$.

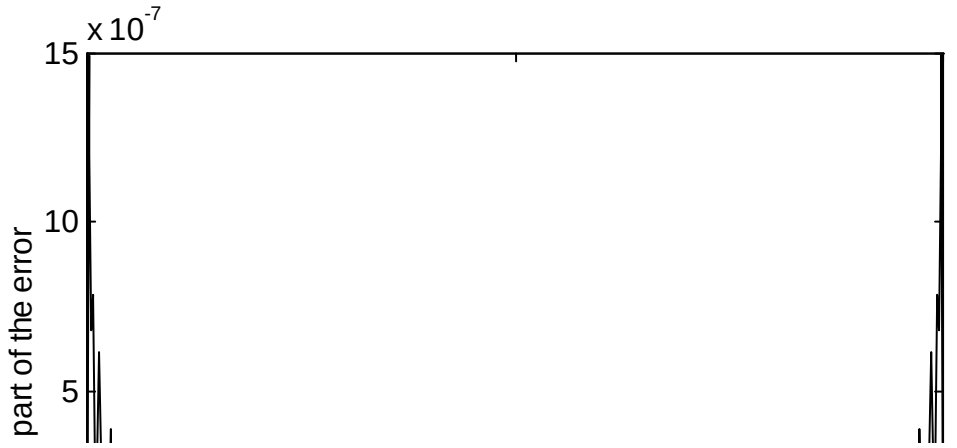

Fig. 11b: The interpolation error for the Morlet wavelet in the second scheme for $|t| \le 5$.